

# Magnetic instability of the orbital-selective Mott phase

Markus Greger, Michael Sekania,\* and Marcus Kollar  
*Theoretical Physics III, Center for Electronic Correlations and Magnetism,  
Institute of Physics, University of Augsburg, 86135 Augsburg, Germany*  
(Dated: October 23, 2021)

We characterize the low-energy physics of the two-orbital Hubbard model in the orbital-selective Mott phase, in which one band is metallic and the other insulating. Using dynamical mean-field theory with the numerical renormalization group at zero temperature, we show that this phase has a ferromagnetic instability for any nonzero Hund's rule exchange interaction, which can be understood in terms of an effective spin-1 Kondo Hamiltonian. The metallic band therefore behaves as a singular Fermi liquid for which the self-energy has a logarithmic singularity at the Fermi energy.

PACS numbers: 71.27.+a, 71.30.+h

In order to explain the properties of most strongly correlated metals, their multi-orbital band structure must be taken into account. In such strongly interacting multi-band systems the local Coulomb interaction acts not only on the electronic charge, as in single-band systems, but also on the spin degrees of freedom. The additional spin-spin interaction is due to the Hund's rule exchange coupling and can lead to a whole array of new complexity which is absent in the single-band case. This relevance of the Hund's rule coupling for the physics of many strongly correlated metals has been discussed on many occasions in recent years [1–3]. This development has led to the classification of so-called *Hund's metals* [3], i.e., itinerant systems in which the Hund's rule coupling is primarily responsible for strongly correlated behavior.

Iron-based superconductors provide an important example for such systems: On the one hand, they are increasingly considered to be strongly correlated because they often exhibit typical correlated behavior such as small coherence scales and significant mass enhancements [1]. On the other hand their density-density interaction is only moderate, so that traditionally they would be regarded as weakly correlated because they are not close to a Mott metal-to-insulator transition (MIT). The MIT itself can be already understood from the paradigmatic single-band Hubbard model, which however does not contain the spin-spin interaction and is therefore unable to describe Hund's metals. Besides modifying the character of strong correlations [4], the complexity introduced by the Hund's rule coupling can also induce rich metallic physics beyond the traditional Fermi-liquid (FL) picture of the single-band Hubbard model in the paramagnetic phase, as well as new quantum phase transitions in addition the Mott MIT.

As we will explicitly show in this paper, the much-studied orbital-selective Mott phase (OSMP) represents precisely such a new genuinely multi-orbital phase for which the Hund's rule coupling plays a crucial role, and which we characterize in this paper (for temperature  $T = 0$ ). The concept of the OSMP was first introduced to explain the metallic properties of  $\text{Ca}_{2-x}\text{Sr}_x\text{RuO}_4$  [5] and

describes cases in which certain bands are Mott insulators while the other bands remain metallic and need not be close to localization. This phase thus provides an interesting chimera between metal and Mott insulator, which has been the subject of many theoretical studies [6–11]. An OSMP was also identified in several other materials. Namely the manganite compound  $\text{La}_{1-x}\text{Sr}_x\text{MnO}_3$  with its localized  $t_{2g}$  and metallic  $e_g$  electrons is regarded as one of the prototypical realizations of the phase [1]. Other examples are FeO and CoO under pressure [12, 13] as well as  $\text{V}_2\text{O}_3$  [14, 15]. Of particular interest is the recent observation of OSMPs in iron pnictides such as  $\text{A}_x\text{Fe}_{2-y}\text{Se}_2$  ( $\text{A}=\text{K}, \text{Rb}$ ) [16, 17] and  $\text{FeSe}_{0.42}\text{Te}_{0.58}$  [18], suggesting the relevance of orbital-selective physics in microscopic models for the pnictides [16, 19, 20]. Significant departures from FL in the OSMP behavior were already established in Ref. 21 and explained by mapping the lattice Hamiltonian onto an effective double-exchange model at low energies. This effective model led to the conjecture of an instability towards ferromagnetism [21], competing with an antiferromagnetic instability [22] due to superexchange between localized spin degrees of freedom. Here we concentrate on the ground-state properties of the OSMP, classify its non-FL nature, and show that the Hund's rule exchange indeed causes a ferromagnetic instability as soon as the OSMP is reached.

*Two-band Hubbard model.* — For our systematic study of the low-energy physics of the OSMP we use its fundamental theoretical model [8, 21], i.e., the two-band Hubbard model with different bandwidths, on-site Hubbard, density-density, and Hund's rule exchange interactions without interorbital hopping, solved in dynamical mean-field theory (DMFT) [23, 24]. The Hamiltonian is given by

$$\begin{aligned} H &= - \sum_{\langle ij \rangle m \sigma} t_m d_{im\sigma}^\dagger d_{jm\sigma} + U \sum_{im} n_{im\uparrow} n_{im\downarrow} + H_J, \\ H_J &= \sum_{i\sigma\sigma'} (U_1 - \delta_{\sigma\sigma'} J) n_{i1\sigma} n_{i2\sigma'} \\ &\quad + \frac{1}{2} J \sum_{im\sigma} d_{im\sigma}^\dagger (d_{im\bar{\sigma}}^\dagger d_{im\bar{\sigma}} + d_{im\bar{\sigma}}^\dagger d_{im\sigma}) d_{im\sigma}. \end{aligned} \quad (1)$$

Here  $i, j$  denote site,  $m = 1, 2$  orbital, and  $\sigma = \uparrow, \downarrow$  spin indices, with bars denoting the respective alternate value. We assume semi-elliptic densities of states with bandwidths  $W_m$ , corresponding, e.g., to scaled nearest-neighbor hopping amplitudes  $t_m = W_m/(4\sqrt{\mathcal{Z}})$  on a Bethe lattice in the limit of infinite coordination number  $\mathcal{Z}$  [24]. We consider half-filled bands and put  $W_2/W_1 = 2$  throughout the paper; other fillings and bandwidth ratios yield qualitatively similar behavior. Note that the Hamiltonian consists of two Hubbard models with the same Hubbard interaction  $U$  which are coupled at each site  $i$  only by  $H_J$  through the interorbital repulsion  $U_1$  and Hund's rule exchange coupling  $J$ . As a consequence, the single-particle Green functions  $G_m(\omega)$  and self-energies  $\Sigma_m(\omega)$  are band-diagonal, whereas the two-particle and higher-order Green functions also have nondiagonal components. Two-particle Green functions will be important for the characterization of ground-state properties in the OSMP and the question of its stability [8, 21]. In the following we treat the charge interaction  $U_1$  and the spin interaction  $J$  as independent parameters because they act in different channels. In most cases we will put  $U_1 = U - 2J$ , valid for  $d$  electrons. Only homogeneous phases are considered. Previously we studied the FL phase of this model (for which  $U$  is so small that both bands are metallic and no phase transition occurs) [25], showing that a small Hund's rule coupling induces the same coherence scale in both bands even though their single-particle spectra are quite different. We use the numerical renormalization group (NRG) [26] to solve the effective DMFT impurity problem, making exponentially small excitation energies accessible, employing the same code and parameters as in Ref. 25. Here we concentrate on the low-energy physics and two-particle quantities at zero temperature, a temperature regime that is notoriously difficult to reach with Quantum Monte Carlo methods but required to study the stability of the phase. In particular we fully characterize the non-FL [21] properties of the itinerant band.

In the OSMP the Hubbard interaction  $U$  is sufficiently strong that the narrow band ( $m = 1$ ) becomes Mott insulating, but sufficiently weak that the wide band ( $m = 2$ ) remains metallic. The obtained one-particle Green functions  $G_m(\omega)$  and self-energies  $\Sigma_m(\omega)$  are very similar to those of two independent single-band Hubbard models [27], one Mott insulating and one metallic, as shown Fig. 1. However, the two bands are not in fact independent, due to the interband coupling terms in the Hamiltonian. This is evident only from two-particle response functions, namely the spin susceptibilities  $\chi_{m,m'}^{\text{sp}}(\omega) = -\text{Im} \langle \langle S_{i,m}^z, S_{i,m'}^z \rangle \rangle_\omega / \pi$  ( $\chi_m^{\text{sp}} \equiv \chi_{m,m}^{\text{sp}}$  denotes the diagonal parts), which exhibit a dominant low-frequency response, see Fig. 2(a). In the single-band Hubbard model this behavior is neither found in the Mott insulating nor in the metallic phase and hence represents a true multi-band effect induced by the interband coupling. In view of the

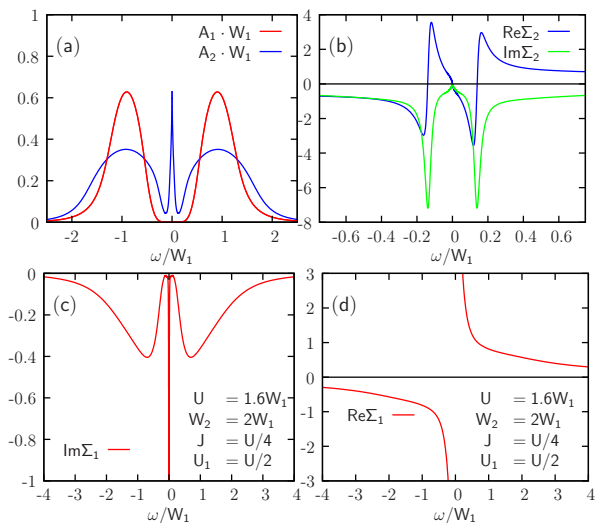


Figure 1: Single-particle quantities in the OSMP, i.e., (a) spectral functions  $A_m(\omega) = -(1/\pi)\text{Im} G_m(\omega)$  and (b,c,d) self-energies  $\Sigma_m(\omega)$ , are qualitatively similar to the single-band Hubbard model in the metallic resp. insulating phase. Note that for the metallic (Fermi-liquid) band,  $A_2(0)$  is pinned to its non-interacting value  $4/(\pi W_2)$  in DMFT [24].

increasing frequency resolution of NRG for  $\omega \rightarrow 0$ , the low-frequency closeup in Fig. 2(b) provides evidence that  $\chi_m^{\text{sp}}$  indeed diverges in the OSMP, suggesting a magnetic instability of the phase at zero temperature.

This striking correlated behavior arises from the Hund's rule exchange interaction  $J$  rather than the density interaction  $U_1$ , as can be seen from Fig. 3 in which either  $J$  or  $U_1$  is set to zero. For  $J = 0$ ,  $U_1 > 0$  the spin susceptibilities are essentially the same as for two decoupled Hubbard models (one Mott insulating and one metallic), i.e., the peaks in  $\chi_2^{\text{sp}}(\omega)$  are finite while  $\chi_1^{\text{sp}}(\omega)$  has a spin gap. Note that the gaps in  $A_1(\omega)$  and  $\chi_1^{\text{sp}}(\omega)$  imply that the Mott-localized spins of the insulating band are decoupled from the rest of the system at small excitation energies. Furthermore the off-diagonal susceptibility  $\chi_{12}^{\text{sp}}(\omega)$  vanishes exactly for  $J = 0$ , because its

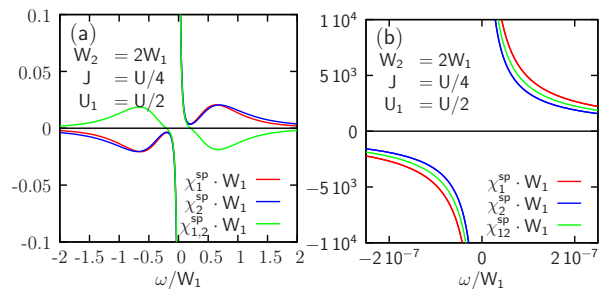


Figure 2: Spin susceptibilities in the OSMP (same parameters as Fig. 1) for large (a) and vanishing frequencies (b). All three susceptibilities diverge for  $\omega \rightarrow 0$ . The low-frequency cutoff for the spectra in this calculation is  $\omega_c \simeq 10^{-8}W_1$ .

equation of motion contains  $[S_{z,1}, H_J] = -[S_{z,2}, H_J] = J(S_1^+ S_2^- - S_2^+ S_1^-)$ . Hence the two bands are essentially decoupled both at the one- and two-particle level. By contrast, for  $U_1 = 0$  and arbitrarily small  $J > 0$  the susceptibilities remain divergent and the system cannot be regarded as the composition of one Mott-insulating and one metallic single-band Hubbard model. Thus the OSMP has a quantum critical point at  $J = 0$ , with  $U_1$  merely modifying its properties quantitatively. We therefore set  $U_1$  to zero in the following and discuss nonzero  $U_1$  again at the end.

*Minimal two-impurity Anderson model.*— In order to understand the divergent susceptibilities in Figs. 2 and 3(d), we construct a minimal low-energy model that captures the low-energy physics of the spin degrees of freedom in the OSMP. As described below, such divergences are found in the two-impurity Anderson model (TIAM) [2, 25] in which one impurity spin is localized (unhybridized with the host) and the other itinerant (hybridized), in analogy to the OSMP. Its Hamiltonian is given by [28, 29]

$$H_{\text{TIAM}} = \sum_{\mathbf{k}m\sigma} \epsilon_{\mathbf{k}m} c_{\mathbf{k}m\sigma}^\dagger c_{\mathbf{k}m\sigma} + \sum_{m\sigma} \epsilon_m n_{m\sigma} + \sum_{\mathbf{k}m\sigma} (V_{\mathbf{k}m} c_{\mathbf{k}m\sigma}^\dagger d_{m\sigma} + \text{h.c.}) + H_J^{\text{loc}}, \quad (2)$$

where the local interaction  $H_J^{\text{loc}}$  has the same form as  $H_J$ , but without the index  $i$ . This is also the type of TIAM onto which the Hamiltonian (1) is mapped in DMFT, subject to two self-consistency conditions for  $G_m(\omega)$ . The coupling of the two impurity sites to the baths is characterized by the hybridization functions  $\Delta_m(\omega) = \sum_{\mathbf{k}} |V_{\mathbf{k}m}|^2 / (\omega + i0 - \epsilon_{\mathbf{k}m})$ . We consider a TIAM in which the hybridization function for the itinerant band  $\Delta_2(\omega)$  is constant, while for the Mott-insulating band

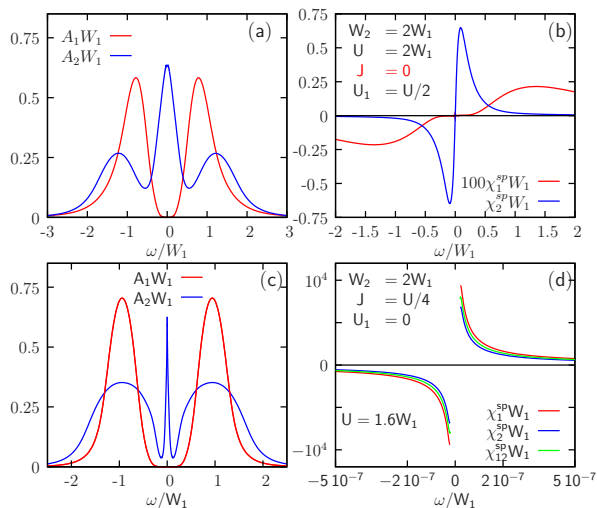


Figure 3: Comparison of the cases  $J = 0$ ,  $U_1 \neq 0$  (a, b) and  $J \neq 0$ ,  $U_1 = 0$  (c, d).

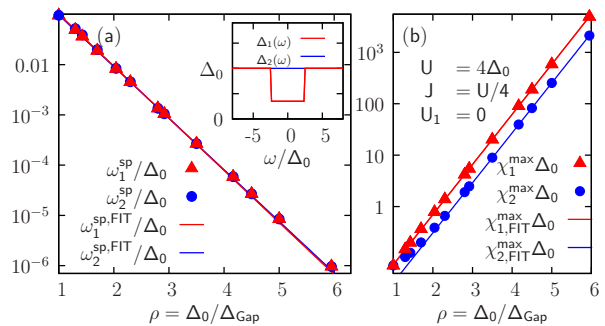


Figure 4: (a) Exponential decay of the quasiparticle coherence scale  $\omega_i^{\text{sp}}/\Delta_0 = A_i \exp(-B_i \rho)$  as a function of the pseudogap strength  $\rho \equiv \Delta_0/\Delta_{\text{gap}}$  ( $A_1 = 0.1030$ ,  $B_1 = 2.3626$ ,  $A_2 = 0.1095$ ,  $B_2 = 2.3844$ ). (b) Amplitude  $\chi_i^{\text{max}}$  of the spin susceptibilities. The exponential dependence  $\chi_i^{\text{max}} \Delta_0 = C_i \exp(D_i \rho)$  for  $\rho \gtrsim 2$  follows from the exponential dependence of the coherence scale (Kondo temperature)  $\omega_1^{\text{sp}} \approx \omega_2^{\text{sp}}$  which is the only scale that determines  $\chi_i^{\text{sp}}(\omega)$  for small  $\omega$  in the limit  $\omega_1^{\text{sp}} \rightarrow 0$  ( $C_1 = 0.0785$ ,  $D_1 = 2.2441$ ,  $C_2 = 0.0353$ ,  $D_2 = 2.2364$ ). The inset in (a) shows the hybridization functions (3). Parameters for both plots given in (b).

the hybridization function  $\Delta_1(\omega)$  has a (pseudo-)gap, i.e., a piecewise constant hybridization function which is smaller in a low- $\omega$  range,

$$\Delta_1(\omega) = \Delta_0 - (\Delta_0 - \Delta_{\text{gap}})\Theta(\omega_0 - |\omega|), \quad (3a)$$

$$\Delta_2(\omega) = \Delta_0, \quad (3b)$$

where  $\Theta(x)$  is the unit step function and we choose  $\omega_0 = 2.5\Delta_0$  for the gap interval (see inset in Fig. 4a). (We verified that other, qualitatively similar choices for the TIAM yield comparable results.) This model interpolates between a standard TIAM ( $\Delta_{\text{gap}} = 0$ ) and a TIAM with a fully gapped band ( $\Delta_{\text{gap}} = \Delta_0$ ) and mimics the self-consistent hybridization functions obtained from DMFT.

The low-energy behavior of the spin susceptibilities are characterized by the energy scale of spin fluctuations in the TIAM, i.e., the extrema  $\omega_m^{\text{sp}}$  of  $\chi_m^{\text{sp}}(\omega)$  and the peak amplitudes  $\chi_m^{\text{max}} \equiv \chi_m^{\text{sp}}(\omega_m^{\text{sp}})$  [25]. These are shown in Fig. 4 as functions of  $\rho \equiv \Delta_0/\Delta_{\text{gap}}$ , a parameter that measures how small the hybridization is inside the gap interval. Both characteristic quantities exhibit an exponential dependence on  $\rho$ . Note that the coherence scales of *both* bands vanish exponentially and are approximately equal,  $\omega_1^{\text{sp}} \approx \omega_2^{\text{sp}}$ , although the gap is opened *in only one* of the two hybridization functions. This correlation is reminiscent of the Hund's-rule-induced proportionality of the two self-energies in the FL phase of the model [25]. Furthermore, the corresponding peak amplitudes  $\chi_m^{\text{max}}$  increase exponentially as the gap is opened. We thus conclude that for a fully gapped TIAM ( $\rho = \infty$ ) the low-energy scale  $\omega_m^{\text{sp}}$  is zero while the spin susceptibilities  $\chi_m^{\text{sp}}$  diverge. In Fig. 5 we plot  $\text{Im}\Sigma_1(\omega)$ ,  $A_m(\omega)$ , and  $\chi_{m,m'}^{\text{sp}}(\omega)$  for this fully gapped case. We observe a striking resemblance to the corresponding DMFT results

in the OSMP (Figs. 1a,c and 3b). Again we verified that other choices for the interactions  $J$  and  $U_1$  lead to the same qualitative behavior (not shown). The only important prerequisites for the divergences in  $\chi_{m,m'}^{\text{SP}}(\omega)$  are the low-energy gap in  $\Delta_1(\omega)$  and a nonzero Hund's rule coupling  $J > 0$ .

*Effective two-impurity Kondo model and singular Fermi liquid.*— The behavior of  $\chi_{m,m'}^{\text{SP}}(\omega)$  can be understood from the Kondo limit ( $U \gg \Delta_0$ ) of the TIAM, i.e., [2, 25]

$$H_{2\text{IK}} = \sum_{\mathbf{k}m\sigma} \epsilon_{\mathbf{k},m} n_{\mathbf{k}m\sigma} + \sum_m J_m \mathbf{s}_m \cdot \mathbf{S}_m - J \mathbf{S}_1 \cdot \mathbf{S}_2. \quad (4)$$

Here  $\mathbf{S}_m$  describes the spins of the two impurity orbitals and  $\mathbf{s}_m$  are the spins of the host electrons (with momentum distributions  $n_{\mathbf{k}m\sigma}$ ) at the impurity site. The superexchange coupling  $J_m > 0$  between  $\mathbf{S}_m$  and  $\mathbf{s}_m$  is antiferromagnetic; the Hund's rule coupling  $J > 0$  (from (1)) provides the coupling  $-J \mathbf{S}_1 \cdot \mathbf{S}_2$  of the impurity spins.

In the TIAM, the dependence of  $\chi_m^{\text{SP}}(\omega)$  on  $\rho$  at low energies is due to spin fluctuations which are described by (4): when  $\Delta_1(\omega)$  is fully gapped ( $\rho \rightarrow \infty$ ), the antiferromagnetic coupling  $J_1 \propto \Delta_{\text{gap}}$  between the spin  $\mathbf{S}_1$  and its host band vanishes. The ferromagnetic coupling of the two impurity spins will then produce a spin-1 object for any nonzero  $J > 0$ , i.e., it will favor the triplet sector of  $\mathbf{S} = \mathbf{S}_1 + \mathbf{S}_2$ . This composite spin-1 is coupled to the electrons from bath  $\Delta_2(\omega)$  but decoupled from bath  $\Delta_1(\omega)$ , i.e., it is only partially screened. In the self-consistent DMFT solution of the lattice model (1) a similar situation occurs in the OSMP: the gap in the self-consistent bath  $\Delta_1(\omega)$  implies that the spins of the gapped band  $A_1(\omega)$  are coupled to the rest of the system only through  $J$ , leading to triplet formation across orbitals 1 and 2.

Both the fully gapped TIAM and the OSMP of the lattice model (1) are thus described by an underscreened spin-1 Kondo-type model [30], which has an intrinsic instability towards ferromagnetism. This quantum critical behavior is manifest in divergent spin susceptibilities [31–33], i.e., the density of states for magnetic excitations becomes infinite at  $\omega = 0$ . In contrast to a standard

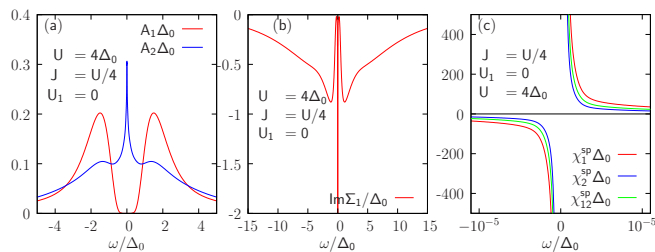


Figure 5: Spectral functions  $A_m(\omega)$  (a), self-energy  $\text{Im} \Sigma_1(\omega)$  of the Mott-insulating band (b) and spin susceptibilities  $\chi_{m,m'}^{\text{SP}}(\omega)$  (c) for the fully gapped TIAM, i.e., for  $\rho = \infty$ . The quantities capture all qualitative features of the self-consistent DMFT results in the OSMP, shown Figs. 1 and 2.

(local) Fermi liquid, the metallic properties of such underscreened models are characterized by a vanishing coherence scale and are referred to as *singular Fermi liquids* (SFL) [33–35]. The self-energy of SFLs is given at low frequencies by [36]

$$\text{Im} \Sigma_{\text{SFL}}(\omega) = a_1 \log^{-2} |\omega/T_0| + \mathcal{O}(\log^{-4} |\omega/T_0|), \quad (5a)$$

$$\text{Re} \Sigma_{\text{SFL}}(\omega) = a_2 \log^{-3} |\omega/T_0| + \mathcal{O}(\log^{-5} |\omega/T_0|). \quad (5b)$$

The scale  $T_0$  corresponds to the Kondo scale of the underscreened spin-1 impurity, i.e., the energy scale at which the crossover to the unscreened (residual) spin 1/2 occurs [33, 36]. In Fig. 6a and b we show fits of Eqs. (5a) and (5b) to the metallic self-energy  $\Sigma_2(\omega)$  of the DMFT solution, confirming the SFL character of the metallic band in the OSMP. By contrast, the behavior of standard Fermi liquids is observed for  $U_1 > 0$  and  $J = 0$  (Fig. 6b and d).

*Conclusion.*— Using DMFT, we established that the metallic state in the OSMP of the two-band Hubbard model is a singular Fermi liquid and clarified the long-standing question of quantum criticality towards ferromagnetism of the phase, which was first discussed in the context of an approximate double-exchange Hamiltonian [21]. We found that a ferromagnetic instability is induced by any nonzero Hund's rule coupling  $J > 0$ , and since it results from the effective Kondo physics it will depend only weakly on details such as the noninteracting band structure. As a consequence, a pure OSMP ground state of (1) is unstable, also in more realistic multi-band Hubbard models or in correlated materials.

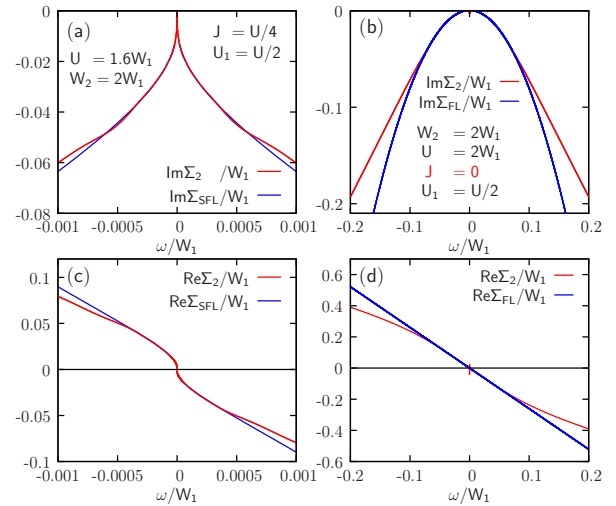


Figure 6: Low-energy behavior of the metallic self-energy  $\text{Im} \Sigma_2(\omega)$  ( $\text{Re} \Sigma_2(\omega)$ ) in the OSMP (a, c) and the corresponding fits to the SFL expressions Eqs. (5a) and (5b); fit parameters are  $a_1 = 0.907 W_1$ ,  $a_2 = 4.372 W_1$ ,  $T_0^{(\text{Im})} = 0.040 W_1$ ,  $T_0^{(\text{Re})} = 0.038 W_1$ . We emphasize the limited accuracy of  $T_0^{(\text{Im,Re})}$  due to the logarithmic nature of the fits. Note the contrast to the case  $J = 0$  (b, d) with the standard FL behavior ( $\text{Im} \Sigma(\omega) \propto -\omega^2$  and  $\text{Re} \Sigma(\omega) \propto -\omega$ ).

However, any weak interband hybridization is expected to turn the OSMP into a Fermi liquid with a small coherence scale [1], which will lead to an orbital-selective Mott transition at finite temperature, as observed in the iron pnictide  $\text{Rb}_x\text{Fe}_{2-y}\text{Se}_2$  [16, 17]. In any case, the ground state of a system with *selective Mottness* [19] will be different from the (unstable) OSMP of the idealized Hamiltonian (1). In particular, superexchange processes between neighboring lattice sites can induce antiferromagnetic order, which will compete with the ferromagnetic instability due to the Hund's rule exchange.

*Acknowledgments.*— We are grateful to Wilhelm Appelt, Liviu Chioncel, Shintaro Hoshino, and Dieter Vollhardt for useful discussions. This work was supported in part by the Deutsche Forschungsgemeinschaft through TRR 80.

---

\* Current address: Theoretical Physik I, University of Würzburg, Am Hubland, 97074 Würzburg, Germany.

- [1] A. Georges, L. de Medici, and J. Mravlje, *Ann. Rev. Cond. Matter Phys.* **4**, 137 (2013).
- [2] L. de' Medici, J. Mravlje, and A. Georges, *Phys. Rev. Lett.* **107**, 256401 (2011).
- [3] K. Haule and G. Kotliar, *New J. Phys.* **11**, 025021 (2009).
- [4] K. Byczuk, J. Kuneš, W. Hofstetter, and D. Vollhardt, *Phys. Rev. Lett.* **108**, 087004 (2012).
- [5] V. Anisimov, I. Nekrasov, D. Kondakov, T. Rice, and M. Sigrist, *Eur. Phys. J. B* **25**, 191 (2002).
- [6] L. de' Medici, S. R. Hassan, M. Capone, and X. Dai, *Phys. Rev. Lett.* **102**, 126401 (2009).
- [7] A. Koga, N. Kawakami, T. M. Rice, and M. Sigrist, *Phys. Rev. Lett.* **92**, 216402 (2004).
- [8] L. de' Medici, A. Georges, and S. Biermann, *Phys. Rev. B* **72**, 205124 (2005).
- [9] A. Liebsch, *Phys. Rev. Lett.* **95**, 116402 (2005).
- [10] E. Jakobi, N. Blümer, and P. van Dongen, *Phys. Rev. B* **87**, 205135 (2013).
- [11] R. Arita and K. Held, *Phys. Rev. B* **72**, 201102 (2005).
- [12] A. O. Shorikov, Z. V. Pchelkina, V. I. Anisimov, S. L. Skornyakov, and M. A. Korotin, *Phys. Rev. B* **82**, 195101 (2010).
- [13] L. Huang, Y. Wang, and X. Dai, *Phys. Rev. B* **85**, 245110 (2012).
- [14] M. S. Laad, L. Craco, and E. Müller-Hartmann, *Phys. Rev. B* **73**, 045109 (2006).
- [15] A. I. Poteryaev, J. M. Tomczak, S. Biermann, A. Georges, A. I. Lichtenstein, A. N. Rubtsov, T. Saha-Dasgupta, and O. K. Andersen, *Phys. Rev. B* **76**, 085127 (2007).
- [16] M. Yi, D. H. Lu, R. Yu, S. C. Riggs, J.-H. Chu, B. Lv, Z. K. Liu, M. Lu, Y.-T. Cui, M. Hashimoto, S.-K. Mo, Z. Hussain, C. W. Chu, I. R. Fisher, Q. Si, and Z.-X. Shen, *Phys. Rev. Lett.* **110**, 067003 (2013).
- [17] Z. Wang, M. Schmidt, J. Fischer, V. Tsurkan, M. Greger, D. Vollhardt, A. Loidl, and J. Deisenhofer, (2013), arXiv:1309.6084 .
- [18] D. Arčon, P. Jeglič, A. Zorko, A. Potočnik, A. Y. Ganin, Y. Takabayashi, M. J. Rosseinsky, and K. Prassides, *Phys. Rev. B* **82**, 140508 (2010).
- [19] L. de' Medici, G. Giovannetti, and M. Capone, (2012), arXiv:1212.3966 .
- [20] N. Lanatà, H. U. R. Strand, G. Giovannetti, B. Hellsing, L. de' Medici, and M. Capone, *Phys. Rev. B* **87**, 045122 (2013).
- [21] S. Biermann, L. de' Medici, and A. Georges, *Phys. Rev. Lett.* **95**, 206401 (2005).
- [22] Y. Koyama, A. Koga, N. Kawakami, and P. Werner, *Physica B: Cond. Matter* **404**, 3267 (2009).
- [23] W. Metzner and D. Vollhardt, *Phys. Rev. Lett.* **62**, 324 (1989).
- [24] A. Georges, G. Kotliar, W. Krauth, and M. J. Rozenberg, *Rev. Mod. Phys.* **68**, 13 (1996).
- [25] M. Greger, M. Kollar, and D. Vollhardt, *Phys. Rev. Lett.* **110**, 046403 (2013).
- [26] R. Bulla, T. A. Costi, and T. Pruschke, *Rev. Mod. Phys.* **80**, 395 (2008).
- [27] R. Bulla, *Phys. Rev. Lett.* **83**, 136 (1999).
- [28] A. Koga, N. Kawakami, T. Rice, and M. Sigrist, *Physica B: Cond. Matter* **359-361**, 1366 (2005).
- [29] K. Inaba and A. Koga, *Phys. Rev. B* **73**, 155106 (2006).
- [30] P. Nozieres and A. Blandin, *J. Phys. (France)* **41**, 193 (1980).
- [31] P. Mehta, N. Andrei, P. Coleman, L. Borda, and G. Zarand, *Phys. Rev. B* **72**, 014430 (2005).
- [32] A. Posazhennikova, B. Bayani, and P. Coleman, *Phys. Rev. B* **75**, 245329 (2007).
- [33] W. Koller, A. C. Hewson, and D. Meyer, *Phys. Rev. B* **72**, 045117 (2005).
- [34] C. Varma, Z. Nussinov, and W. van Saarloos, *Phys. Rep.* **361**, 267 (2002).
- [35] P. Coleman and C. Pépin, *Phys. Rev. B* **68**, 220405 (2003).
- [36] C. J. Wright, *Theoretical studies of underscreened Kondo physics in quantum dots*, Ph.D. thesis, Oxford University (2011).